Phosphocholine accumulation and PHOSPHO1 depletion promote adipose tissue thermogenesis

Mengxi Jiang[a,1], Tony E. Chavarria[a], Bingbing Yuan[a], Harvey F. Lodish[a,b,c,2], and Nai-Jia Huang[a,1,2]

[a]Whitehead Institute for Biomedical Research, Cambridge, MA 02142; [b]Department of Biology, Massachusetts Institute of Technology, Cambridge, MA 02142; and [c]Department of Biological Engineering, Massachusetts Institute of Technology, Cambridge, MA 02142

Contributed by Harvey Lodish, May 5, 2020 (sent for review September 24, 2019; reviewed by Christopher B. Newgard and Philipp E. Scherer)

Phosphocholine phosphatase-1 (PHOSPHO1) is a phosphocholine phosphatase that catalyzes the hydrolysis of phosphocholine (PC) to choline. Here we demonstrate that the PHOSPHO1 transcript is highly enriched in mature brown adipose tissue (BAT) and is further induced by cold and isoproterenol treatments of BAT and primary brown adipocytes. In defining the functional relevance of PHOPSPHO1 in BAT thermogenesis and energy metabolism, we show that PHOSPHO1 knockout mice are cold-tolerant, with higher expression of thermogenic genes in BAT, and are protected from high-fat diet-induced obesity and development of insulin resistance. Treatment of mice with the PHOSPHO1 substrate phosphocholine is sufficient to induce cold tolerance, thermogenic gene expression, and allied metabolic benefits. Our results reveal a role of PHOSPHO1 as a negative regulator of BAT thermogenesis, and inhibition of PHOSPHO1 or enhancement of phosphocholine represent innovative approaches to manage the metabolic syndrome.

PHOSPHO1 | adipose | thermogenesis | phosphocholine

Thermogenesis of brown and beige adipose tissues dissipates energy as heat to combat cold and is mediated by uncoupling protein 1 (UCP1)-mediated proton transport across the mitochondrial inner membrane (1–5). An alternative pathway of brown adipose tissue (BAT) activation involves mechanisms independent of UCP1, such as ATP-dependent Ca^{2+} cycling (6–8) and creatine-dependent ADP/ATP futile cycling (8–10). Thermogenesis is highly energy-consuming (11–15) and can be exploited for weight management. Cold exposure and β-adrenergic agonists activate thermogenesis both in "classic" brown adipocytes and in the inducible beige adipocytes that emerge within white adipose tissue (WAT) following certain stimuli (16–20). The detection of BAT in human adults sparked an interest in augmenting energy metabolism through enhancing thermogenic activity in brown and beige adipocytes (21–24). However, cold exposure and β-adrenergic agonist administration are not feasible therapies for humans due to impractical regimens and systemic toxicities, respectively. Thus, finding novel mechanisms to promote browning and enhancing BAT thermogenesis is of considerable interest.

Phosphocholine phosphatase-1 (PHOSPHO1) is a phosphocholine phosphatase that catalyzes the hydrolysis of phosphocholine (PC) to choline and is required in bone for the generation of inorganic phosphate groups for matrix mineralization (25, 26). Several reports implicate PHOSPHO1 in lipid and energy metabolism. DNA methylation at the PHOSPHO1 locus in DNA from blood cells was negatively associated with future type 2 diabetes risk and positively correlated with high-density lipoprotein levels (27–29); and genome-wide association analysis identified a single nucleotide polymorphism in the PHOSPHO1 gene that is highly associated with obesity (30).

PHOSPHO1 plays a key role in lipid metabolism during red blood cell terminal differentiation (31). A recent study showed that PHOSPHO1 is overexpressed in UCP1 knockout (KO) beige adipocytes and functions downstream in UCP1-independent energy expenditure (9). However, the precise functions of PHOSPHO1 in brown and beige adipocytes are not understood.

Here, we show that PHOSPHO1 is highly enriched in mature BAT and is transcriptionally induced by cold exposure and isoproterenol treatment, both in BAT and primary brown adipocytes. Mice lacking PHOSPHO1 display enhanced thermogenic gene expression and are cold-tolerant, lean, and insulin-sensitive. Treatment with the PHOSPHO1 substrate PC mimicked the PHOSPHO1 KO in inducing cold tolerance, thermogenic gene expression, and metabolic benefits. Our results uncover functions of PHOSPHO1 as a negative, and PC as a positive, regulator of BAT thermogenesis and energy metabolism.

Results

PHOSPHO1 Gene Expression and Function Are Associated with Thermogenesis in BAT. Analyzing the tissue expression pattern of *Phospho1* mRNA from the mouse ENCODE database, we found that PHOSPHO1 is highly enriched in BAT (Fig. 1*A*). Moreover, *Phospho1* mRNA accumulated in brown adipocytes during in vitro differentiation (Fig. 1*B*). We then used real-time-PCR to quantify the expression of *Phospho1* mRNA in various mouse tissues. Consistent with the ENCODE data, PHOSPHO1 is highly enriched in BAT and is also expressed at lower levels in

Significance

Thermogenesis by brown adipose tissue (BAT) dissipates energy as heat and combats obesity. The detection of BAT in human adults sparked an interest in treating metabolic disorders through BAT activation. However, the current browning regimen suffers from patient incompliance and systemic toxicity. We show that phosphocholine phosphatase-1 (PHOSPHO1) is highly enriched in BAT and negatively regulates thermogenesis. PHOSPHO1 knockout mice are cold-tolerant and are protected from high-fat diet-induced obesity and insulin resistance. Phosphocholine, the PHOSPHO1 substrate, induced cold tolerance and allied metabolic benefits in mice. Our results identified a BAT-enriched negative regulator of thermogenesis. Inhibition of PHOSPHO1 or enhancement of phosphocholine may represent innovative approaches to manage obesity and its related metabolic syndrome.

Author contributions: M.J., H.F.L., and N.-J.H. designed research; M.J., T.E.C., B.Y., and N.-J.H. performed research; M.J., T.E.C., B.Y., H.F.L., and N.-J.H. analyzed data; and M.J., H.F.L., and N.-J.H. wrote the paper.

Reviewers: C.B.N., Duke University Medical Center; and P.E.S., University of Texas Southwestern Medical Center.

The authors declare no competing interest.

Data deposition: The data reported in this paper have been deposited in the Gene Expression Omnibus (GEO) database (accession no. GSE129020).

See online for related content such as Commentaries.

[1]M.J. and N.-J.H. contributed equally to this work.

[2]To whom correspondence may be addressed. Email: lodish@wi.mit.edu or njhuang@wi.mit.edu.

This article contains supporting information online at https://www.pnas.org/lookup/suppl/doi:10.1073/pnas.1916550117/-/DCSupplemental.

First published June 17, 2020.

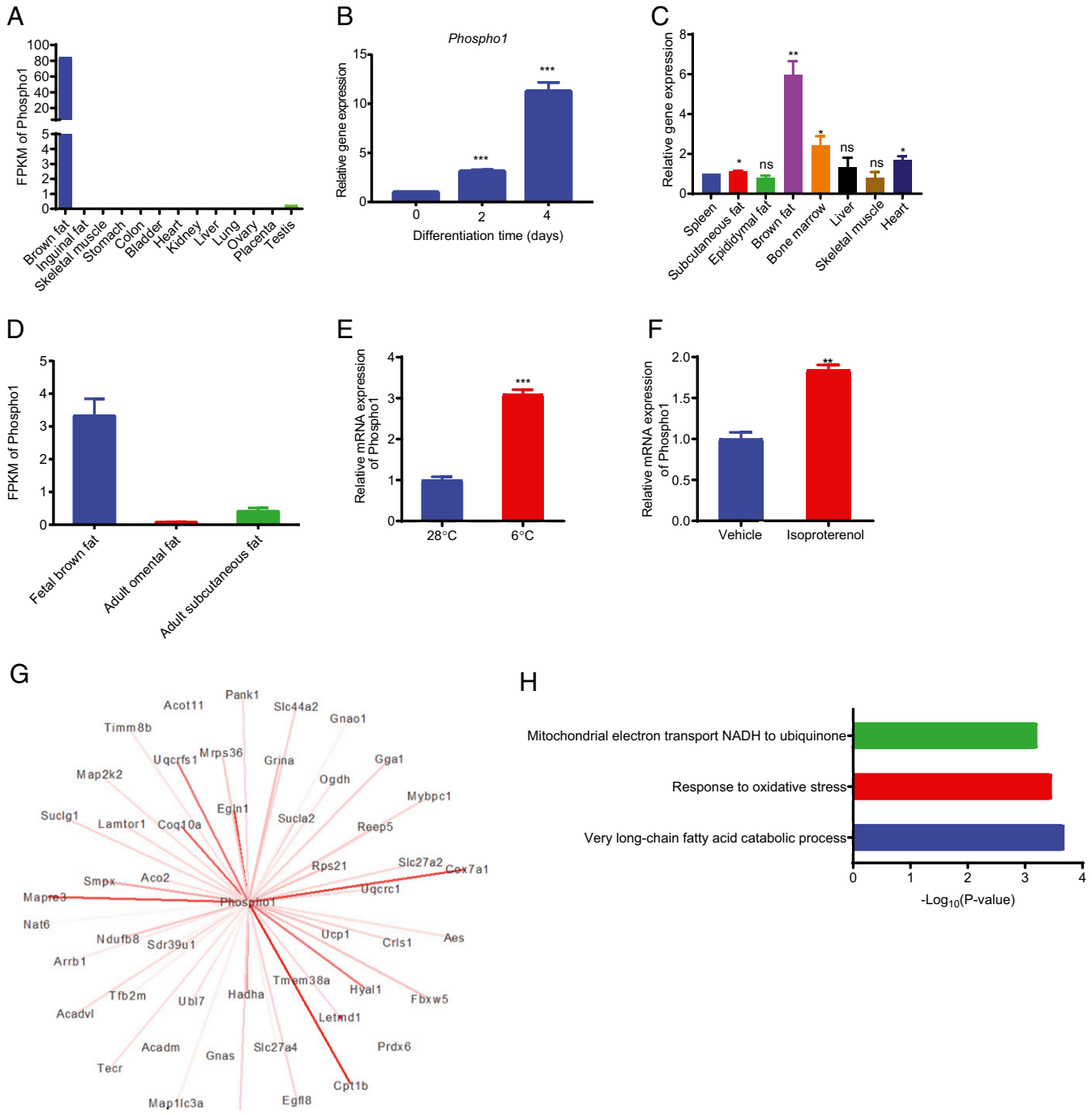

Fig. 1. PHOSPHO1 is predominantly expressed in BAT. (*A*) *Phospho1* mRNA expression from the mouse ENCODE dataset. (*B*) *Phospho1* mRNA expression in WT-1 brown adipocyte cells increases during differentiation ($n = 6$). (*C*) *Phospho1* mRNA expression in different tissues from 7-wk-old mice ($n = 5$). (*D*) *Phospho1* mRNA expression in human adult subcutaneous, omental, and fetal brown adipose tissues (GSE97205). (*E*) *Phospho1* mRNA expression in BAT of mice housed at 6 °C and 28 °C (GSE51080). (*F*) 1 μM Isoproterenol induced *Phospho1* mRNA expression in cultured primary brown adipocytes at 6 d of differentiation ($n = 3$). (*G*) The top 50 PHOSPHO1 coexpressed genes are ranked by the sum of the neighbor's log-likelihood (LLS) scores. *Ucp*1 gene expression is highly associated with PHOSPHO1 expression. (*H*) Top functional pathways of PHOSPHO1 coexpressed genes. ns, nonsignificant; $*P < 0.05$; $**P < 0.01$; $***P < 0.001$. FPKM, fragments per kilobase of transcript per million mapped reads.

inguinal WAT (iWAT), bone marrow, and heart (Fig. 1*C*). The BAT-enriched expression pattern of PHOSPHO1 is not mouse-specific; *Phospho1* mRNA is more highly expressed in thermogenic fetal human brown fat than in adult fat tissues with a lower thermogenic capacity (Fig. 1*D*).

Cold exposure activates BAT thermogenesis. We mined an existing dataset of cold exposure (GSE51080) and found a higher expression of *Phospho1* mRNA in BAT of mice housed at 6 °C compared with mice maintained at 28 °C (Fig. 1*E*). To show that cold treatment indeed induced PHOSPHO1 expression, we harvested the stromal-vascular fraction (SVF) from BAT of mice and differentiated them into mature brown adipocytes. Treatment of these primary mature brown adipocytes with isoproterenol, a β-adrenergic agonist, elevated the mRNA expression

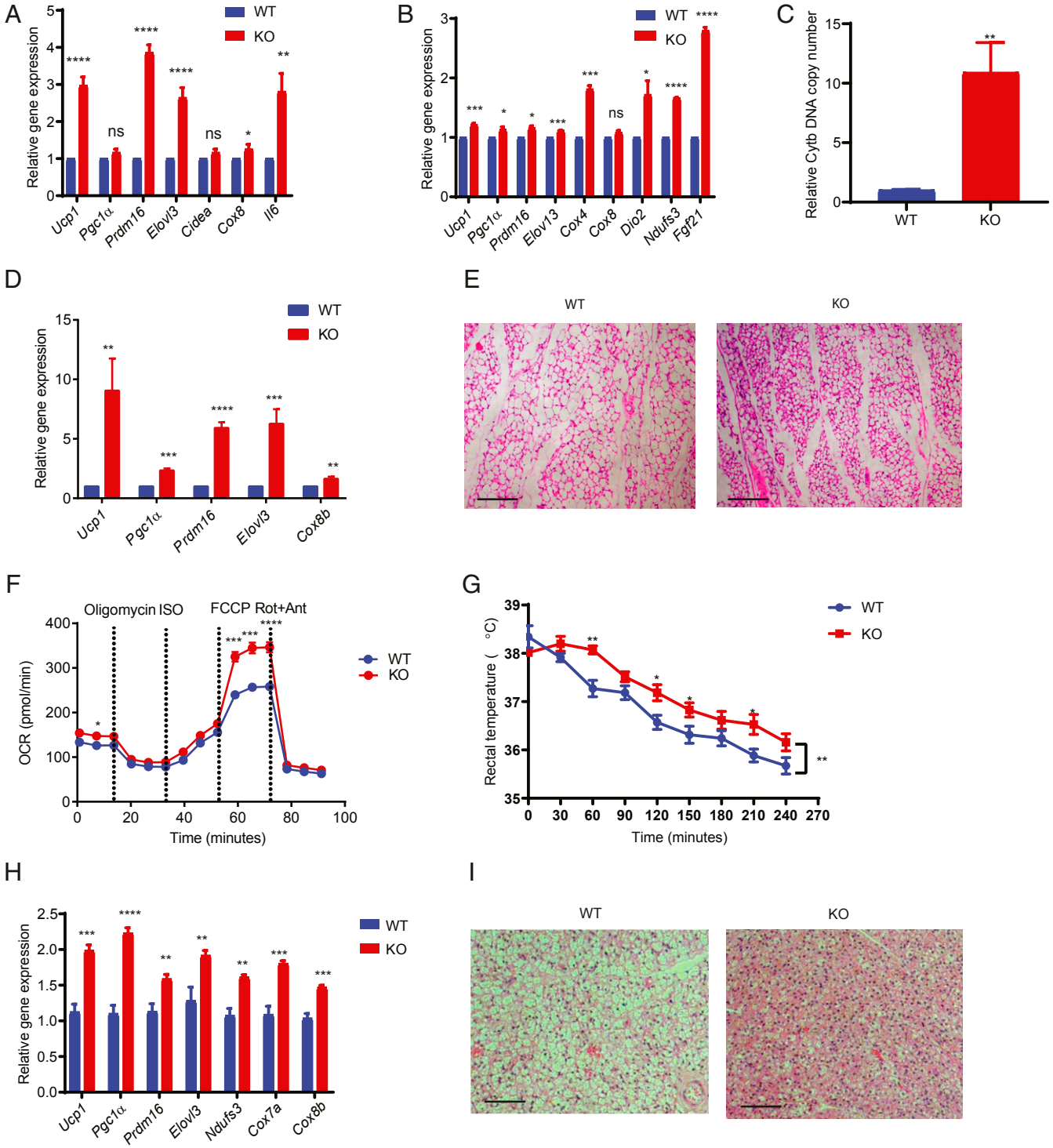

Fig. 2. PHOSPHO1 KO mice have improved thermogenic capacity and are cold-tolerant. (*A*) Thermogenic gene mRNA expression of BAT in 7-wk-old WT and PHOSPHO1 KO mice ($n = 7$ for each genotype). (*B*) Thermogenic gene mRNA expression was elevated in primary cultured brown adipocytes from PHOSPHO1 KO mice at 6 d of differentiation ($n = 4$). (*C*) Higher mitochondrial content in BAT from PHOSPHO1 KO mice. mtDNA Cytb copy number was used to calculate the relative number of mitochondria ($n = 5$). (*D*) mRNA expression in scWAT from 7-wk-old WT and KO mice ($n = 7$ for each genotype). (*E*) H&E stain of scWAT from 7-wk-old WT and KO mice. (Scale bars, 200 μm.) (*F*) Oxygen consumption rate of primary WT and KO brown adipocytes at 6 d of differentiation ($n = 5$). ISO, isoproterenol; FCCP, carbonyl cyanide-4 (trifluoromethoxy) phenylhydrazone; Rot, rotenone; Ant, antimycin. (*G*) Rectal temperature of WT and KO mice upon exposure to 4 °C. Mice were initially housed at 20 °C. ($n = 6$) (*H*) mRNA expression in brown adipose tissue from WT and KO mice exposed to 4 °C for 7 h ($n = 3$). (*I*) H&E stain of BAT from WT and KO mice exposed to 4 °C for 7 h. (Scale bars, 200 μm.) ns, nonsignificant; $^{*}P < 0.05$; $^{**}P < 0.01$; $^{***}P < 0.001$; $^{****}P < 0.0001$.

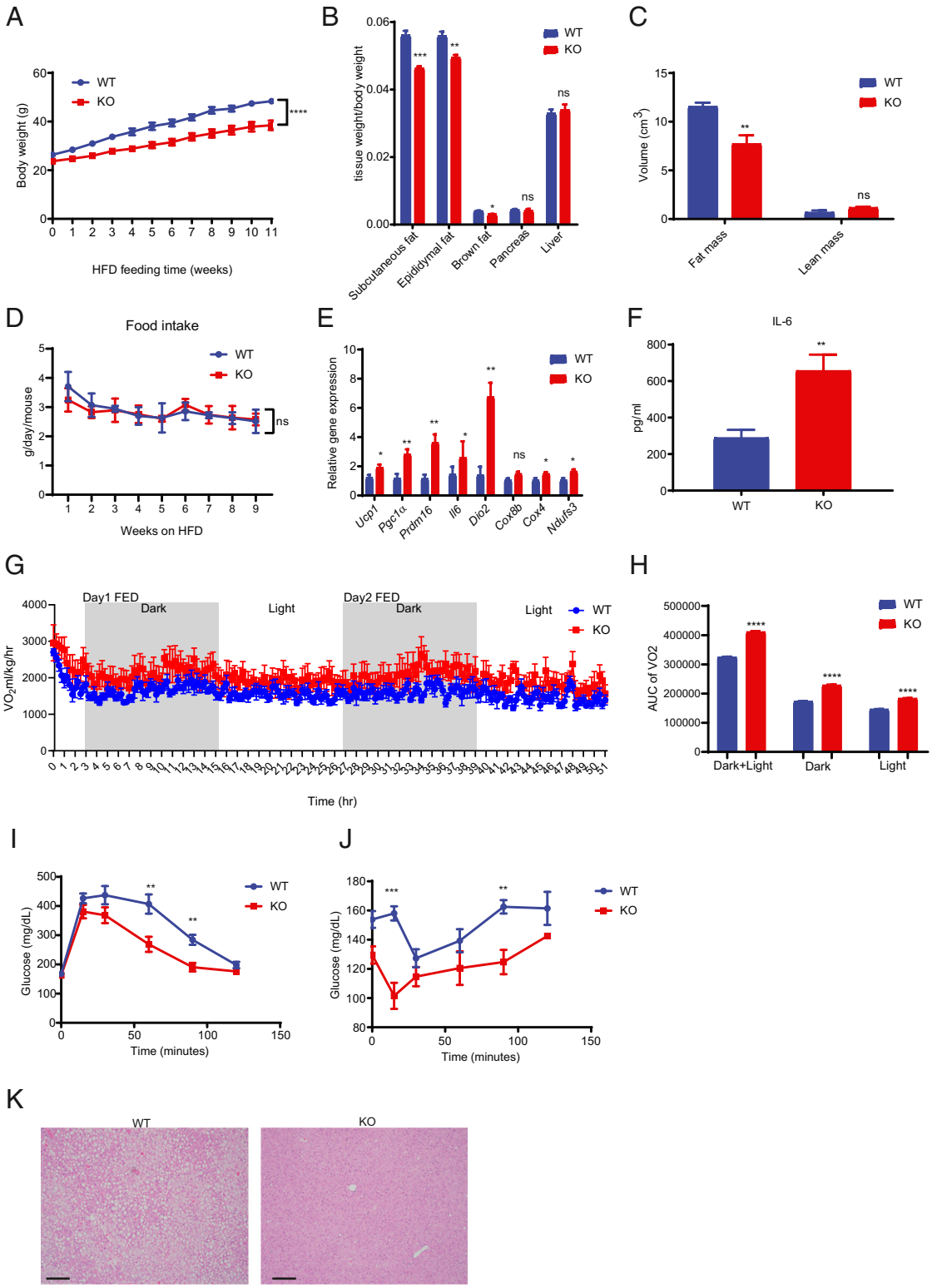

Fig. 3. PHOSPHO1 KO mice display an improved metabolic phenotype upon HFD challenge. (*A*) WT and KO mice were fed an HFD from 6 wk of age for 11 wk ($n = 10$ for each genotype). Body weight was measured weekly. (*B*) Tissue weights from WT and KO mice fed an HFD for 14 wk ($n = 7$). (*C*) Body composition of mice following 14 wk of high-fat feeding ($n = 7$). (*D*) Food intake of HFD-fed mice ($n = 7$). Difference is not significant at each time point. (*E*) mRNA expression in BAT following 14 wk of high-fat feeding ($n = 7$). (*F*) IL-6 concentration in WT and KO serum after 14 wk of HFD ($n = 7$). (*G*) Oxygen consumption of mice fed for 13 wk of HFD ($n = 5$). (*H*) Area under the curve of *G*. (*I*) Glucose tolerance test. Blood glucose was measured after a 1.5 g/kg glucose injection into mice following 12 wk of HFD ($n = 7$). (*J*) ITT. Blood levels were measured after 0.75 U/kg insulin injection into mice following 13 wk of HFD ($n = 7$). (*K*) H&E staining of liver tissue from 14-wk HFD-fed WT and PHOSPHO1 KO mice (Scale bars, 100 μm.) ns, nonsignificant; $^{*}P < 0.05$; $^{**}P < 0.01$; $^{***}P < 0.001$; $^{****}P < 0.0001$.

of PHOSHPO1 (Fig. 1*F*), suggesting the involvement of β-adrenergic signaling in regulating PHOSPHO1 expression in mature brown adipocytes during BAT activation.

To further analyze the function and molecular network of PHOSPHO1, PHOSPHO1-coexpressed genes were extracted from 248 published Gene Expression Omnibus (GEO) series and ranked based on the sum of log-likelihood scores from all PHOSPHO1-coexpression links (32). PHOSPHO1 expression is strongly correlated with that of mitochondrial genes, such as *Ucp1*, *Ndufb8*, *Cox7a1*, *Coq10a*, *Uqcrc1*, and *Cpt1b* (Fig. 1*G*). Gene ontology (GO) analyses of biological processes revealed that genes encoding proteins involved in mitochondrial electron transport, oxidative stress response, and lipid catabolism were highly enriched as PHOSPHO1 coexpressed partners (Fig. 1*H*), which suggest that PHOSPHO1 is likely involved in these functions as well. These results suggest that PHOSPHO1 is an important regulator of brown fat metabolism and thermogenesis.

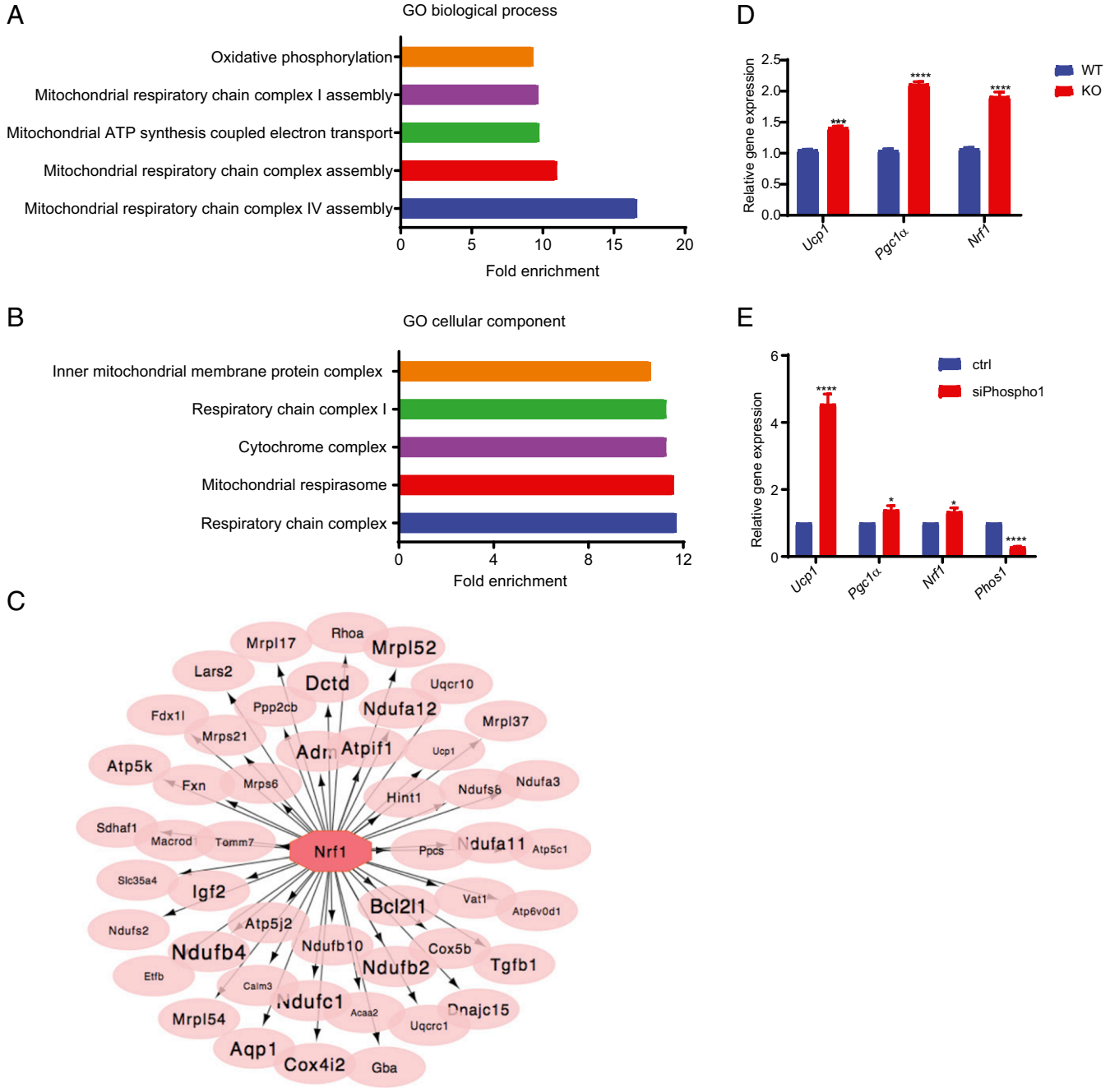

Fig. 4. Differential gene-expression analysis indicates that mitochondrial function- and biogenesis-related genes are enriched in PHOSPHO1 KO BAT compared with WT BAT. (*A*) Functional analysis of differentially expressed genes in KO BAT versus WT BAT (GO biological process, 1.5-fold induction, FDR < 0.06) (*B*) Differentially expressed genes in KO BAT versus WT BAT (GO cellular component). (*C*) Transcription factor association analysis indicates that the transcription factor *Nrf1* is associated with up-regulated genes. (*D*) Higher *Pgc1α* and *Nrf1* mRNA expression in in vitro differentiated primary brown adipocytes isolated from PHOSPHO1 KO mice compared to WT mice ($n = 5$). (*E*) Higher *Nrf1* mRNA expression in cultured PHOSPHO1 knockdown brown adipocyte cells, WT-1, at 7 d of differentiation ($n = 6$). *$P < 0.05$; ***$P < 0.001$; ****$P < 0.0001$.

PHOSPHO1 KO Mice Display Increased BAT Thermogenesis and Are Protected from High-Fat Diet-Induced Obesity and Type 2 Diabetes. The induction of PHOSPHO1 in BAT and primary brown adipocytes by cold exposure and isoproterenol treatment prompted us to investigate whether PHOSPHO1 is involved in BAT thermogenesis. Indeed, we found that PHOSPHO1 negatively regulates thermogenesis.

Ablation of PHOSPHO1 in mice brown adipose tissue (Fig. 2*A*) and in primary brown adipocytes (Fig. 2*B*) induced, at room temperature, the expression of mRNAs encoding a number of thermogenic marker genes, including *Ucp1*, *Pgc1α*, *Prdm16*, *Fgf21*, *Dio2*, *Elovl3*, and *Cidea*. Expression of many mitochondrial genes, including *Cox8b*, *Cox4*, and *Ndufs3*, as well as mitochondrial copy number (Fig. 2*C*), were also elevated in PHOSPHO1 KO BAT and brown adipocytes compared with their WT counterparts. This effect was not limited to BAT, as the induced thermogenic program was also observed in iWAT of PHOSPHO1 KO mice (Fig. 2*D*), together with the appearance of beige adipocytes filled with small lipid droplets in PHOSPHO1 KO iWAT (Fig. 2*E*).

The increased expression of thermogenic genes in PHOSPHO1 KO adipose tissues prompted us to investigate the respiratory activity of isolated brown adipocytes from WT and PHOSPHO1 KO mice. PHOSPHO1 KO brown adipocytes displayed slightly increased basal respiration, and strikingly increased maximal respiration relative to WT brown adipocytes (Fig. 2*F*). Consistent with the increased thermogenic gene expression in and oxygen consumption by KO brown adipocytes, PHOSPHO1 KO mice were better able to sustain their core body temperature compared with WT mice during an acute cold exposure (Fig. 2*G*). The cold-tolerant phenotype in PHOPHO1 KO mice was accompanied with increased thermogenic gene expression in KO BAT assessed after cold exposure (Fig. 2*H*), as well as a more active BAT morphology manifested by reduced cellular lipid stores (Fig. 2*I*). Thus, PHOSPHO1 is a negative regulator of BAT thermogenesis, and depletion of PHOSPHO1 promotes BAT thermogenesis and energy expenditure.

Given the critical role of BAT in energy metabolism, we next tested whether PHOSPHO1 deficiency in mice affects energy metabolism in response to high-fat diet (HFD)-induced obesity and the development of insulin resistance. PHOSPHO1 KO mice gained less body weight than WT mice during 11 wk of HFD treatment (Fig. 3*A*). Tissue weight measurements and body composition analysis showed that the reduced weight gain by PHOSPHO1 KO mice was mainly due to decreased fat mass, as the lean mass was comparable between mice of the two genotypes (Fig. 3 *B* and *C*). Body weight is a balance of energy intake and energy expenditure. Since food intake was comparable between WT and KO mice (Fig. 3*D*), it is likely that, compared with WT mice, the reduced body weight gain in KO mice was caused by increased energy expenditure. Indeed, thermogenic gene expression in KO BAT was higher than in WT BAT in response to an HFD (Fig. 3*E*). IL-6, a BAT-produced cytokine beneficial to glucose homeostasis and energy metabolism (33, 34), was induced in KO BAT (Fig. 3*E*) and the serum IL-6 concentration was correspondingly higher in KO than WT mice (Fig. 3*F*). Consistent with the activation of thermogenic genes, HFD-fed KO mice exhibited an increase in oxygen consumption, both during the night when the mice are active and in the light, compared to their WT counterparts (Fig. 3 *G* and *H*). This explains the slower weight gain by KO mice.

Obesity is closely associated with insulin resistance. We then measured insulin sensitivity in HFD-fed WT and KO mice by an intraperitoneal glucose tolerance test (IPGTT) and an insulin tolerance test (ITT). Consistent with their leaner phenotype, the HFD-fed PHOSPHO1 KO mice showed improved glucose tolerance and insulin sensitivity compared to WT controls, as assessed both by IPGTT and ITT (Fig. 3 *I* and *J*). As noted above, when compared with WT mice, PHOSPHO1 KO mice displayed a higher expression of thermogenic genes in BAT in response to the HFD challenge (Fig. 3*E*). HFD-induced hepatic lipid accumulation was ameliorated in PHOSPHO1 KO mice compared with WT mice (Fig. 3*K*). Together, these results indicate that PHOSPHO1 deficiency in mice leads to improved energy metabolism, glucose homeostasis, and insulin sensitivity during an HFD.

PHOSPHO1 KO BAT Express Increased Numbers of mRNAs Encoding Proteins Essential for Mitochondrial Biogenesis. To determine the molecular basis of the increased BAT thermogenesis and energy metabolism in PHOSPHO1 KO mice, we performed RNA sequencing (RNA-seq) on WT or KO mature BAT depleted of the SVF. We identified 487 up-regulated and 1,349 down-regulated genes (fold-change >1.5, false-discovery rate [FDR] < 0.06) in KO BAT compared with WT BAT. To examine the biological functions of the elevated genes, we performed an enrichment analysis. The biological process GO category revealed mitochondrial respiratory chain complex assembly, mitochondrial ATP synthesis-coupled electron transport, and oxidative phosphorylation as the top up-regulated pathways in PHOSPHO1 KO BAT (Fig. 4*A*). The cellular component GO category revealed the respiratory chain complex and inner mitochondrial membrane protein complex as the top-scoring gene categories (Fig. 4*B*). To identify the putative protein factors controlling this transcriptional response, we performed a motif analysis of the up-regulated genes using the Broad Molecular Signatures Database (MSigDB). Binding sites of the nuclear respiratory factor-1 (Nrf1), the key factor mediating mitochondrial biogenesis (35–37), was designed as one of the top-scoring motifs (Fig. 4*C*). Accordingly, we showed that the level of *Nrf1* mRNA was elevated in PHOSPHO1 KO primary brown adipocytes, and PHOSPHO1 knocked down brown adipocytes cell lines (Fig. 4 *D* and *E*), compared to WT controls, consistent with increased the mitochondrial copy number in KO BAT (Fig. 2*C*). This result showed that the transcriptional programs leading to mitochondrial biogenesis are increased in PHOSPHO1 KO BAT.

PC Promotes BAT Activation. The substrate of PHOSPHO1, PC, is produced by hydrolysis of the phospholipid phosphatidylcholine (PtdCho) or by phosphorylation of choline. We observed a higher ratio of PC to choline in the serum of PHOSPHO1 KO mice compared to WT mice (Fig. 5*A*). To understand if PHOSPHO1's function in BAT is related to phosphatidylcholine hydrolysis, we performed lipidomic analysis of cultured brown adipocytes differentiated for 0, 2, and 4 d. The total amount of lipid, relative to protein, increased approximately twofold during brown adipocyte differentiation (Fig. 5*B*) in parallel with major changes in the lipid composition (*SI Appendix*, Fig. S1). The amount of PC increased markedly during the first 2 d of differentiation and then decreased, while the amount of PtdCho, relative to the total amount of lipid, continuously decreased during differentiation (Fig. 5 *C* and *D*). Taken together, these data suggest that PtdCho hydrolysis induced by PHOSPHO1 causes the transient increased PC accumulation in differentiating brown adipocytes.

We hypothesize that PC accumulation is correlated with the activity of brown adipocytes. Indeed, PC is among the top 10% increased metabolites in BAT upon acute cold-induced activation of BAT thermogenesis (38) (Fig. 5*E*) and increased phosphatidylcholine hydrolysis, generating PC, in BAT upon cold exposure was seen in previous studies (39, 40).

To determine whether an increase in PC mediates the increased thermogenesis and energy metabolism observed in PHOSPHO1 KO mice, we treated cultured brown adipocytes with PC and found elevated expression of thermogenic genes together with reduced ATP content (Fig. 6 *A* and *B*). This effect

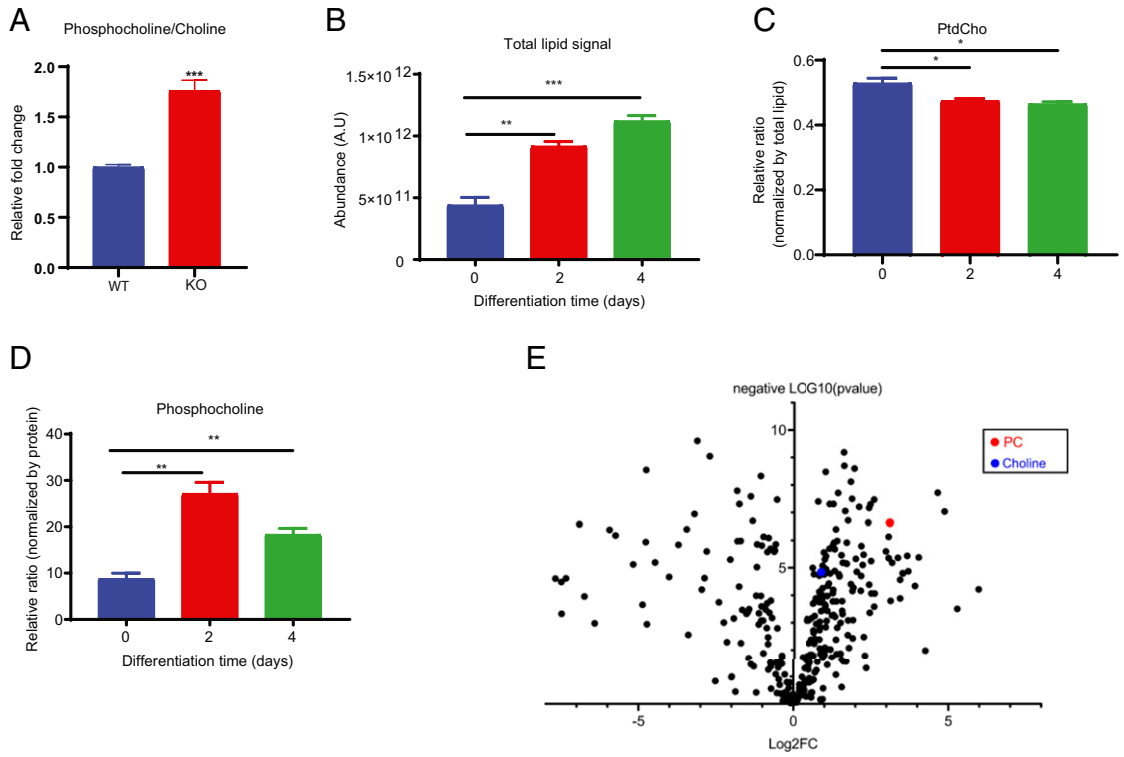

Fig. 5. PC is enriched in differentiated and active BAT. (*A*) Ratio of PC to choline in the serum of PHOSPHO1 KO mice and WT mice. (*B*) Total lipid increases during differentiation of primary brown adipocytes ($n = 3$). (*C*) Decreased phosphatidylcholine composition during primary brown adipocyte differentiation ($n = 3$). Data are from *SI Appendix*, Fig. S1 positive ion panel. (*D*) PC is accumulated in brown adipocytes early during differentiation ($n = 3$). (*E*) Increased PC in BAT from mice following a 3-h exposure to 4 °C relative to BAT from mice kept at thermoneutrality. Data were extracted from supplementary table S3 in Mills et al. (38). Log2FC = $\log_2$ of fold-change between BAT from cold-exposed mice versus thermoneutrality. Negative log10(*P* value) = negative $\log_{10}$ of the *P* value. Each dot represents each changed metabolite and PC is labeled in red. $^*P < 0.05$; $^{**}P < 0.01$; $^{***}P < 0.001$.

was not limited to brown adipocytes since PC treatment also enhanced expression of thermogenic genes in primary white adipocytes (Fig. 6*C*). *Phospho1* mRNA expression was induced upon PC treatment, suggesting substrate-induced up-regulation of the *Phospho1* gene. Consistent with elevated expression of thermogenic and mitochondrial genes, PC treatment enhanced mitochondrial copy number (Fig. 6*D*), as well as basal, isoproterenol-mediated, and maximal oxygen consumption in mature brown adipocytes (Fig. 6*E*). This effect was specific to mature brown adipocytes, as the basal respiration rate in brown preadipocytes was not affected by PC treatment (Fig. 6*F*).

Consistent with induction of thermogenesis by PC, in vivo administration of PC to WT mice enhanced the expression of Ucp1 in BAT (Fig. 6*G*), attenuated the core body temperature decline in response to acute cold exposure (Fig. 6*H* and *SI Appendix*, Fig. S2), and improved glucose homeostasis in HFD-fed mice as assessed by IPGTT (Fig. 6*I*). Together, our results demonstrate that PC promotes thermogenic activity in both BAT and iWAT and mimicked the metabolic benefits seen in PHOSPHO1 KO mice.

Discussion

PHOSPHO1, a PC phosphatase that catalyzes the hydrolysis of PC to choline, is induced during differentiation of BAT and its expression is further induced by cold and isoproterenol treatments of BAT and primary brown adipocytes. Paradoxically, we show that PHOSPHO1 is a negative regulator of thermogenesis since depletion of PHOSPHO1 promotes BAT thermogenesis and energy expenditure. PHOSPHO1 KO mice are cold-tolerant with higher expression of thermogenic genes in BAT, and are protected from HFD-induced obesity, fatty liver, and development of insulin resistance. Treatment of both cultured adipocytes and mice with the PHOSPHO1 substrate, PC, is sufficient to induce cold tolerance, thermogenic gene expression, and allied metabolic benefits.

Of all of the tissues tested in mice, PHOSPHO1 is most highly expressed in BAT. Similarly, the expression of PHOSPHO1 in human fetal BAT is highest among all human adipose tissues. Thus, it is likely that BAT is the primary effector tissue of PHOSPHO1 function, and that the effects of inhibiting PHOSPHO1 occur mainly in BAT. The induction of thermogenic genes and browning morphology in iWAT in PHOSPHO1 KO mice suggests that iWAT could also contribute to the induced thermogenesis in PHOSPHO1 KO mice upon cold exposure and HFD treatment. However, since PHOSPHO1 is depleted in all tissues, we cannot exclude the possibility that other tissues or cell types—such as the liver, muscle, or the sympathetic nervous system mediating brown fat activation—may participate in the metabolic benefits observed in PHOSPHO1 KO mice. Future studies using tissue-specific PHOSPHO1 KO mice may enable a better understanding of the target tissues mediating the metabolic actions of PHOSPHO1 in vivo.

Nonetheless, our data show that BAT is a major target of PHOSPHO1 depletion, triggering elevated mitochondrial and thermogenic gene expression, oxygen consumption, and mitochondrial biogenesis, the latter evidenced by an increase in mitochondrial DNA copy number. Indeed, Nrf1 is a key transcription factor mediating mitochondrial biogenesis (35–37) and Nrf1 transcripts were elevated in PHOSPHO1 KO BAT and KO brown adipocytes. Supporting the role of Nrf1 in mediating the effects of

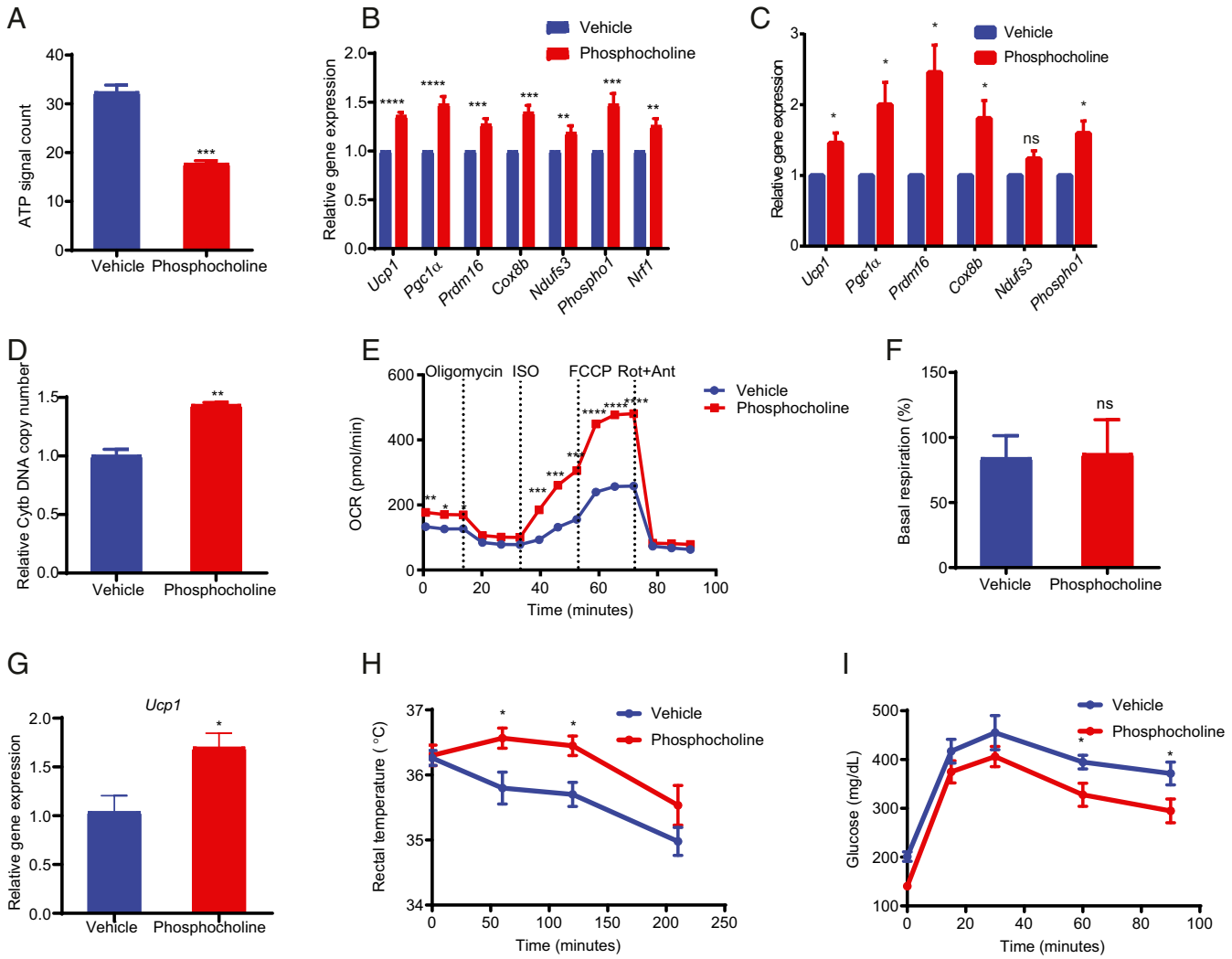

Fig. 6. PC treatment reproduced the improved metabolic phenotype of PHOSPHO1 KO mice. (*A*) ATP content in primary brown adipocytes following 25 μM PC addition at 6 d of differentiation ($n = 3$). (*B*) 50 μM PC induced thermogenic gene expression in the brown adipocyte cell line WT-1 at 7 d of differentiation ($n = 6$). (*C*) 25 μM PC induced thermogenic gene expression in primary subcutaneous white adipocytes at 6 d of differentiation ($n = 3$). (*D*) More mitochondria in PC-treated differentiated WT-1 brown adipocyte cells ($n = 3$). (*E*) PC treatment enhanced basal, isoproterenol-mediated, and maximal oxygen consumption in mature brown adipocytes ($n = 5$). (*F*) 25 μM PC does not change basal respiration in primary brown preadipocytes ($n = 5$). (*G*) Expression of Ucp1 in BAT 24 h after PC injection as determined by real-time PCR. (*H*) The effect of subcutaneously Injected 50 mg/kg PC on the rectal temperature of 8-wk-old mice kept at room temperature when they were subsequently transferred to a 4 °C cold exposure ($n = 5$). PC was injected 24 h and 10 min before the cold exposure. (*I*) Subcutaneously injected 50 mg/kg PC improved glucose tolerance in 14-wk-old mice with 9 wk of HFD ($n = 8$); 1.5 g/kg glucose were injected ($n = 8$). See *SI Appendix*, Fig. S2 for the response to other PC doses. ns, nonsignificant; *$P < 0.05$; **$P < 0.01$; ***$P < 0.001$; ****$P < 0.0001$.

PHOSPHO1 inhibition, we identified Nrf1 binding sites as one of the top-scoring motifs potentially regulating expression of induced genes in PHOSPHO1 KO BAT. The exact role of Nrf1 in regulating PHOSPHO1 KO-induced BAT thermogenesis needs to be further elucidated by loss-of-function studies.

PC is a specific substrate of PHOSPHO1 (26). At least some of the beneficial metabolic benefits of the PHOSPHO1 KO likely resulted from PC accumulation, as evidenced by PC-induced cold tolerance, glucose tolerance, and thermogenic gene expression in BAT. The induction of PHOSPHO1 upon PC treatment may act to hydrolyze the accumulated PC and maintain PC homeostasis, which could explain the elevated levels of PHOSPHO1 and PC (38) in BAT of cold-exposed mice. Given that induction of PHOSPHO1 leads to hydrolysis of PC to choline, and thus reduces the half-life of PC, chemically modified versions of PC resistant to PHOSPHO1-mediated hydrolysis will be necessary to develop the therapeutic potential of PC. Increased hydrolysis of PtdCho and accumulation of PC in BAT upon cold exposure was seen in previous studies (38–40), suggesting that phosphatidylcholine is hydrolyzed to form PC during BAT activation. PC accumulation may also serve as a metabolic signature of BAT activation. However, we cannot exclude the possibility that choline kinase-catalyzed conversion of choline to PC also contributes to PC accumulation inside BAT cells. Further studies elucidating these and other aspects of PC metabolism in brown adipocytes will be important to understand the regulation of thermogenesis induced by PC.

A better understanding of the mechanism of PC-induced thermogenesis could reveal new avenues toward thermogenic activation of BAT; such studies are underway in our laboratories. PC is reported to be bound by the C-reactive protein in triggering innate immunity, and is an agonist of nicotinic acetylcholine receptors in inhibiting the release of IL-1β from monocytes (41, 42). Whether these binding partners execute some of PC's function in thermogenesis is unknown. PC is used

to provide glycine for protein synthesis in erythroblasts (31), and it is possible that PC is converted to a specific metabolite that mediates thermogenesis.

Taken together, our results reveal a role of PC as a positive regulator of BAT thermogenesis, and suggest that inhibition of PHOSPHO1 or enhancement of PC levels represent potential approaches to treat diseases related to the metabolic syndrome.

Materials and Methods

Mice. Except for PHOSPHO1 WT and KO groups, all C57BL/6J male mice were either bred in house or obtained from Jackson Laboratories (stock #000664). PHOSPHO1 KO and WT mice were back-crossed to C57BL/6 background as described previously, and genotyping of PHOSPHO1 mice was performed as described previously (31). All mice were maintained at a 12/12-h light/dark cycle at 20 °C. All animal procedures were approved by the Committee on Animal Care at the Massachusetts Institute of Technology (MIT).

Isolation and Differentiation of Preadipocytes of BAT and iWAT, and Differentiation of Immortalized Brown Preadipocyte Cells. The protocol was previously described (43). Briefly, interscapular BAT and subcutaneous (inguinal) WAT (scWAT) were harvested from 4-wk-old male mice and minced in Dulbecco's Modified Eagle's Medium (DMEM) with 10% fetal bovine serum (FBS). The minced adipose tissues were digested with HBSS (Gibco, #14175-095) supplemented with 2% BSA (Sigma-Aldrich, #A7906) and 0.2% collagenase A (Roche, #10103578001) at 37 °C for 30 min. The SVF was separated from the mature adipocytes by centrifugation at 700 × *g* for 5 min and plated in proliferation medium at 37 °C with 5% CO_2 (Table 1). These cells were cultured and differentiated (2-d postconfluence, d0), as shown in Table 1. The differentiation medium of primary white adipocytes was the same as for primary brown adipocytes, except for the addition of T3. The WT-1 cell line (the immortalized brown preadipocyte cell line) was a gift from Yu-Hua Tseng, Joslin Diabetes Center, Harvard Medical School, Boston, MA. These cells were cultured and differentiated (2-d postconfluence) as shown in Table 1. The medium was changed every 2 d until analysis. Phosphocholine chloride was purchased from Sigma Aldrich #P037 and solutions in water were made fresh.

siRNA Transfection. On day 4 of differentiation, WT-1 cells were forward-transfected twice with 10-nM siRNA pools, which are mixtures of three siRNAs targeted on the same gene (OriGene), using 10 μL/mL Lipofectamine RNAiMAX. The cultures were analyzed on 7-d differentiated cells. PHOSPHO1 siRNA (OriGene #SR407660) and Nrf1 siRNA (Origene# SR416910). For primary brown adipocytes, cells were reverse-transfected as described previously (44). Briefly, mature adipocytes were trypsinized with 0.25% trypsin for 20 min and plated on top of the preincubated siRNA-RNAiMAX mix. The final concentration of siRNA was 50 nM.

HFD Treatment. WT or PHOSPHO1 KO male mice after genotyping were fed an HFD (Research Diets #D12331) beginning at 4 or 5 wk of age; the same number of mice were placed in a large cage and the food was replaced weekly. Beginning during the first week, the food intake of each group was measured daily. Body weight was measured every week in a blinded manner. For glucose tolerance test, 7-h fasted mice were injected with glucose (1.5 g/kg body weight, intraperitoneally) in 0.9% sterile NaCl solution. For ITTs, 7-h fasted mice were injected with insulin (Humulin R, Lilly #0002-8215-01 [HI-210[, 0.75 U/body weight, intraperitoneally). Blood glucose was measured from the tail vein by a Contour blood glucose meter (Bayer). Mice in Fig. 3 *D*, *G*, and *H* were fed an HFD at 16-wk-old. Oxygen consumption was measured by the Comprehensive Laboratory Animal Monitoring System (CLAMS) in the animal physiology core at the Joslin Diabetes Center after each mouse was acclimated in an individual chamber for 24 h. CLAMS data were analyzed using the Columbus Instruments CLAX 2.3 software.

Cold Exposure. WT or PHOSPHO1 KO male mice on a chow diet were transferred from 20 °C to a cold environment (4 °C) with food restriction. The core (rectal) body temperature of mice was measured by a microprobe thermometer (Physitemp, Model BAT-12) in a blinded manner (43).

Measure Mass Volume. Lean and fat volume was monitored using a GE Healthcare eXplore microCT 120 device (250-μm resolution, 70 kV, 50-mA tube current, with 32-ms exposure time). Volumetric microCT images were acquired and reconstructed using GE eXplore software. Data were post processed (Gaussian smoothing) and analyzed using MicroView (Parallax Innovations, microview.parallax-innovations.com/) with manually drawn regions-of-interest. The assay was performed and analyzed by investigators who were blinded to the genotype of the mice and done in the Animal Imaging and Preclinical Testing Core at the Koch Institute for Integrative Cancer Research of MIT.

Seahorse Assays. Primary or immortalized brown adipocytes were plated into 24 or 96 wells with 0.5% gelatin (Sigma-Aldrich #G1890) -coated Seahorse microplate and cells were plated in XF media (Sigma #D5030 medium powder, 1.85 g NaCl and 600 μL phenol red [0.5%] in 1 L) containing 5 mM glucose and 2 mM L-glutamine adjusted to pH 7.4. The microplate was incubated at 37 °C in a non-CO_2 incubator for 1 h before measuring.

Table 1. Adipogenesis protocol and reagents

		Differentiation medium		
Cell type	Proliferation medium	Day 0	Day 2	Day 4 and after
Primary brown adipocytes	DMEM/F12 (LifeTechnologies/Gibco #12634028)	DMEM/F12	DMEM/F12	DMEM (Sigma, #56499C)
	10% Heat inactivated newborn calf serum (HI NCBS, LifeTechnologies/Gibco, #26010-074)	10% FBS	10% FBS	10% FBS
		850 nM Insulin (Sigma-Aldrich #I1882)	160 nM Insulin	
		0.5 μM Dexamethasone (Sigma-Aldrich #D4902)		
		250 μM 3-isobutyl-1-methylxanthine (IBMX, Sigma-Aldrich #I5879)	1 nM T3	
		1 μM Rosiglitazone (Cayman Chemical #71742)		
		1 nM 3,3,5-triiodo-L-thyronine (T3, VWR #100567-778)		
WT-1 cell line	DMEM	DMEM	DMEM	DMEM
	10% FBS	10% FBS (Sigma-Aldrich F2442)	10% FBS	10% FBS
		5 μg/mL Insulin (Sigma-Aldrich #I1882)	5 μg/mL Insulin	
		1 μM Dexamethasone (Sigma-Aldrich #D490)	0.5 μM Rosiglitazone	
		0.5 mM IBMX (Sigma-Aldrich #I5879)		
		0.5 μM Rosiglitazone (Cayman Chemical #71742)		

DMEM, Dulbecco's Modified Eagle's Medium; FBS, fetal bovine serum.

Table 2. Primer sequences

Name	Forward	Reverse
Gapdh	GCAAAGTGGAGATTGTTGCCAT	CCTTGACTGTGCCGTTGAATTT
18S	GTAACCCGTTGAACCCCATT	CCATCCAATCGGTAGTAGC
Ucp-1	CTTTGCCTCACTCAGGATTGG	ACTGCCACACCTCCAGTCATT
Pgc1α	CCCTGCCATTGTTAAGACC	TGCTGCTGTTCCTGTTTTC
Prdm16	CAGCACGGTGAAGCCATTC	GCGTGCATCCGCTTGTG
Elovl3	TTCTCACGCGGGTTAAAAATGG	GAGCAACAGATAGACGACCAC
Cidea	TGACATTCATGGGATTGCAGAC	GGCCAGTTGTGATGACTAAGAC
Cox8b	GAACCATGAAGCCAACGACT	GCGAAGTTCACAGTGGTTCC
Dio2	CAGTGTGGTGCACGTCTCCAATC	TGAACCAAAGTTGACCACCAG
Ndufs3	CAGGGATCACACCAATGCAC	AGTCAATGGGTGTCAGCTCA
Fgf21	GTGTCAAAGCCTCTAGGTTTCTT	GGTACACATTGTAACCGTCCTC
Cox7a1	GCTCTGGTCCGGTCTTTTAGC	GTACTGGGAGGTCATTGTCGG
Nrf1	GTTGGATGAGTACACGACGC	GAATTAACCTCCTGTGGCGC
IL-6	TAGTCCTTCCTACCCCAATTTCC	TTGGTCCTTAGCCACTCCTTC
PHOSPHO1	GGCGATTTGTTGCAGTTCATA	GAGGATGCGGCGGAATAAA
Cox4	ACCAAGCGAATGCTGGACAT	GGCGGAGAAGCCCTGAA

Extracellular acidification rates and oxygen consumption rates were measured on a Seahorse Bioscience XF24–3 or XF96 Extracellular Flux Analyzer. 1 μM oligomycin and FCCP, 0.5 μM Rotenone and antimycin, and 1 μM isoproterenol were used during the measurement. In the PC treatment assay, cells were pretreated with 25 μM PC for 24 h.

Measure Serum IL-6 and Cellular ATP. Blood was collected into a BD microtainer (BD #365967) and the tubes were centrifuged at 3,000 rpm for 10 min. Serum was collected from supernatant of the tubes and measured for IL-6 concentration by Mouse IL-6 Quantikine ELISA Kit (R&D# M6000B) according to the manufacturer's instructions. Cellular ATP content was measured by ATPlite Luminescence Assay kit (Perkin-Elmer # 6016943).

RNA-Seq. RNA samples from 6-wk-old WT or Phosho1 KO mature BAT were extracted using QIazol reagent and RNAeasy kit (Qiagen #74104). The mRNA library was prepared using KAPAHypermRNA kit and samples were run by an Illumina HISEQ sequencer with single-end sequencing (50 cycles). Sequences were aligned to mouse genome (mm9) using STAR (23104886) with Ensembl gene model v67. After reads were checked for strandness with the infer_experiment.py function from RSeQC (22743226), only reverse-stranded reads were assigned to genes with STAR. Genes not expressed (not a single sample with at least one read) were removed, and deferentially expressed genes were identified with DESeq2 (25516281). RNA-seq data were submitted to the National Center for Biotechnology Information GEO (GSE129020).

Real-Time Quantitative PCR. RNA samples were extracted using QIazol reagent and RNAeasy kit (Qiagen #74104) and 1 μg RNA was reverse-transcribed using Invitrogen superscript III reverse transcriptase (Invitrogen#1808093). qPCR was performed by QuantStudio 6 system from Thermo-Fisher and *18S* or *Gapdh* was used for -ΔΔCT normalization. Primer sequences are listed in Table 2.

Mitochondrial Copy Number. For mtDNA analysis, tissues were homogenized and total DNA was extracted with DNeasy Blood &Tissue Kit (Qiagen). mtDNA was amplified using primers specific for the mitochondrial cytochrome *b*(*CytB*) gene and normalized to genomic DNA by amplification of the large ribosomal protein p0 (*36B4*) nuclear gene according to D'Antona et al. (45).

Histology. Fresh tissues of BAT and scWAT were isolated and fixed in 10% neutral buffered formalin solution (Sigma-Aldrich #HT5014) overnight in a cold room and replaced with 70% ethanol before sending to The Hope Babette Tang Histology Core Facility at the Koch Institute of MIT. After embedding the tissues in paraffin, slide sections were prepared and stained with H&E following established protocols at the Histology Core Facility. Slides were pictured using Zeiss Axiophot upright microscope and Axiovision software.

Metabolomics. For metabolomics, 15 μL of serum samples were mixed with 95 μL MeOH, 190 μL LC/MS grade DCM, and 60 μL LC/MS grade water containing internal standards. The mixture was vortexed at 4 °C for 10 min and spun at 8,000 × *g* for 10 min at 4 °C. Other samples were washed in cold 0.9% NaCl, and resuspend in −20 °C, 600 μL LC/MS grade methanol containing 17 isotope-labeled internal standards. Subsequently, 300 μL LC/MS grade water and −20 °C, 400 μL LC/MS grade chloroform were added. Samples were vortexed at 4 °C 10 min and spun at 14,000 × *g* for 10 min at 4 °C. The top layer (polar metabolite) and bottom layer (lipid metabolite) were analyzed with LC/MS at the Metabolite Profiling Core Facility at the Whitehead Institute. The methods of polar and lipid metabolite profiling by LC/MS was described in a previous paper (46).

Statistics. All analysis data were presented as mean ± SEM unless specified otherwise. Prism was used to calculate the statistical significance. Unless mentioned, an unpaired two-tailed Student's *t* test was used to calculate the *P* values. Figs. 2*F* and 3*A* was analyzed via ANOVA. $P < 0.05$ was considered significant. $*P < 0.05$; $**P < 0.01$; $***P < 0.001$; $****P < 0.0001$.

Data Availability. Data relevant to this paper are included in the figures or *SI Appendix*. Protocols are described in *Materials and Methods* and RNA-seq data were submitted to the National Center for Biotechnology Information GEO (GSE129020).

ACKNOWLEDGMENTS. We thank the Histology, Bioinformatics, and Genome Core facilities and Metabolite Profiling Core at the Whitehead and the Koch Institute; members of the H.F.L. laboratory, especially Sally Winther and Marko Knoll, for fruitful discussions; Ferenc Reinhardt for mouse husbandry; Dr. Yu-Hua Tseng for providing WT-1 cells; Dr. Colin Farquharson and Dr. José Luis Millán for providing the PHOSPHO1 knockout mice for rederivation; and Allen Clermont and Meghan Halpin at Joslin Diabetes Center for Comprehensive Laboratory Animal Monitoring System measurement. This work was sponsored by Grant NIH/DK047618 (to H.F.L.) and an American Heart Association fellowship (to M.J.).

1. K. D. Garlid, M. Jabůrek, P. Jezek, The mechanism of proton transport mediated by mitochondrial uncoupling proteins. *FEBS Lett.* **438**, 10–14 (1998).
2. H. Aquila, T. A. Link, M. Klingenberg, The uncoupling protein from brown fat mitochondria is related to the mitochondrial ADP/ATP carrier. Analysis of sequence homologies and of folding of the protein in the membrane. *EMBO J.* **4**, 2369–2376 (1985).
3. D. G. Nicholls, R. M. Locke, Thermogenic mechanisms in brown fat. *Physiol. Rev.* **64**, 1–64 (1984).
4. J. Nedergaard *et al.*, UCP1: The only protein able to mediate adaptive non-shivering thermogenesis and metabolic inefficiency. *Biochim. Biophys. Acta* **1504**, 82–106 (2001).
5. S. Enerbäck *et al.*, Mice lacking mitochondrial uncoupling protein are cold-sensitive but not obese. *Nature* **387**, 90–94 (1997).
6. K. Ikeda *et al.*, UCP1-independent signaling involving SERCA2b-mediated calcium cycling regulates beige fat thermogenesis and systemic glucose homeostasis. *Nat. Med.* **23**, 1454–1465 (2017).
7. N. C. Bal *et al.*, Sarcolipin is a newly identified regulator of muscle-based thermogenesis in mammals. *Nat. Med.* **18**, 1575–1579 (2012).
8. A. M. Bertholet *et al.*, Mitochondrial patch clamp of beige adipocytes reveals UCP1-positive and UCP1-negative cells both exhibiting futile creatine cycling. *Cell Metab.* **25**, 811–822.e4 (2017).

9. L. Kazak *et al*., A creatine-driven substrate cycle enhances energy expenditure and thermogenesis in beige fat. *Cell* **163**, 643–655 (2015).
10. L. Kazak *et al*., Genetic depletion of adipocyte creatine metabolism inhibits diet-induced thermogenesis and drives obesity. *Cell Metab.* **26**, 693 (2017).
11. K. L. Townsend, Y. H. Tseng, Brown fat fuel utilization and thermogenesis. *Trends Endocrinol. Metab.* **25**, 168–177 (2014).
12. A. Fedorenko, P. V. Lishko, Y. Kirichok, Mechanism of fatty-acid-dependent UCP1 uncoupling in brown fat mitochondria. *Cell* **151**, 400–413 (2012).
13. M. Ahmadian *et al*., Desnutrin/ATGL is regulated by AMPK and is required for a brown adipose phenotype. *Cell Metab.* **13**, 739–748 (2011).
14. E. P. Mottillo, A. E. Bloch, T. Leff, J. G. Granneman, Lipolytic products activate peroxisome proliferator-activated receptor (PPAR) α and δ in brown adipocytes to match fatty acid oxidation with supply. *J. Biol. Chem.* **287**, 25038–25048 (2012).
15. A. Bartelt *et al*., Brown adipose tissue activity controls triglyceride clearance. *Nat. Med.* **17**, 200–205 (2011).
16. N. Petrovic *et al*., Chronic peroxisome proliferator-activated receptor gamma (PPARgamma) activation of epididymally derived white adipocyte cultures reveals a population of thermogenically competent, UCP1-containing adipocytes molecularly distinct from classic brown adipocytes. *J. Biol. Chem.* **285**, 7153–7164 (2010).
17. J. Wu *et al*., Beige adipocytes are a distinct type of thermogenic fat cell in mouse and human. *Cell* **150**, 366–376 (2012).
18. J. Ishibashi, P. Seale, Medicine. Beige can be slimming. *Science* **328**, 1113–1114 (2010).
19. J. Wu, P. Cohen, B. M. Spiegelman, Adaptive thermogenesis in adipocytes: Is beige the new brown? *Genes Dev.* **27**, 234–250 (2013).
20. I. G. Shabalina *et al*., UCP1 in brite/beige adipose tissue mitochondria is functionally thermogenic. *Cell Rep.* **5**, 1196–1203 (2013).
21. J. Nedergaard, T. Bengtsson, B. Cannon, Unexpected evidence for active brown adipose tissue in adult humans. *Am. J. Physiol. Endocrinol. Metab.* **293**, E444–E452 (2007).
22. A. M. Cypess *et al*., Identification and importance of brown adipose tissue in adult humans. *N. Engl. J. Med.* **360**, 1509–1517 (2009).
23. W. D. van Marken Lichtenbelt *et al*., Cold-activated brown adipose tissue in healthy men. *N. Engl. J. Med.* **360**, 1500–1508 (2009).
24. K. A. Virtanen *et al*., Functional brown adipose tissue in healthy adults. *N. Engl. J. Med.* **360**, 1518–1525 (2009).
25. A. J. Stewart *et al*., The presence of PHOSPHO1 in matrix vesicles and its developmental expression prior to skeletal mineralization. *Bone* **39**, 1000–1007 (2006).
26. S. J. Roberts, A. J. Stewart, P. J. Sadler, C. Farquharson, Human PHOSPHO1 exhibits high specific phosphoethanolamine and phosphocholine phosphatase activities. *Biochem. J.* **382**, 59–65 (2004).
27. T. Dayeh *et al*., DNA methylation of loci within ABCG1 and PHOSPHO1 in blood DNA is associated with future type 2 diabetes risk. *Epigenetics* **11**, 482–488 (2016).
28. T. Willmer, R. Johnson, J. Louw, C. Pheiffer, Blood-based DNA methylation biomarkers for type 2 diabetes: Potential for clinical applications. *Front. Endocrinol. (Lausanne)* **9**, 744 (2018).
29. J. C. Chambers *et al*., Epigenome-wide association of DNA methylation markers in peripheral blood from Indian Asians and Europeans with incident type 2 diabetes: A nested case-control study. *Lancet Diabetes Endocrinol.* **3**, 526–534 (2015).
30. Y. Wu *et al*., Genetics of obesity traits: A bivariate genome-wide association analysis. *Front. Genet.* **9**, 179 (2018).
31. N. J. Huang *et al*., Enhanced phosphocholine metabolism is essential for terminal erythropoiesis. *Blood* **131**, 2955–2966 (2018).
32. S. Yang *et al*., COEXPEDIA: Exploring biomedical hypotheses via co-expressions associated with medical subject headings (MeSH). *Nucleic Acids Res.* **45**, D389–D396 (2017).
33. K. I. Stanford *et al*., Brown adipose tissue regulates glucose homeostasis and insulin sensitivity. *J. Clin. Invest.* **123**, 215–223 (2013).
34. K. Timper *et al*., IL-6 improves energy and glucose homeostasis in obesity via enhanced central IL-6 trans-signaling. *Cell Rep.* **19**, 267–280 (2017).
35. N. Gleyzer, K. Vercauteren, R. C. Scarpulla, Control of mitochondrial transcription specificity factors (TFB1M and TFB2M) by nuclear respiratory factors (NRF-1 and NRF-2) and PGC-1 family coactivators. *Mol. Cell. Biol.* **25**, 1354–1366 (2005).
36. M. J. Evans, R. C. Scarpulla, NRF-1: A trans-activator of nuclear-encoded respiratory genes in animal cells. *Genes Dev.* **4**, 1023–1034 (1990).
37. K. Vercauteren, R. A. Pasko, N. Gleyzer, V. M. Marino, R. C. Scarpulla, PGC-1-related coactivator: Immediate early expression and characterization of a CREB/NRF-1 binding domain associated with cytochrome c promoter occupancy and respiratory growth. *Mol. Cell. Biol.* **26**, 7409–7419 (2006).
38. E. L. Mills *et al*., Accumulation of succinate controls activation of adipose tissue thermogenesis. *Nature* **560**, 102–106 (2018).
39. M. D. Lynes *et al*., Cold-activated lipid dynamics in adipose tissue highlights a role for cardiolipin in thermogenic metabolism. *Cell Rep.* **24**, 781–790 (2018).
40. J. Sanchez-Gurmaches *et al*., Brown fat AKT2 is a cold-induced kinase that stimulates ChREBP-mediated de novo lipogenesis to optimize fuel storage and thermogenesis. *Cell Metab.* **27**, 195–209.e6 (2018).
41. J. E. Volanakis, M. H. Kaplan, Specificity of C-reactive protein for choline phosphate residues of pneumococcal C-polysaccharide. *Proc. Soc. Exp. Biol. Med.* **136**, 612–614 (1971).
42. K. Richter *et al*., Phosphocholine—An agonist of metabotropic but not of ionotropic functions of α9-containing nicotinic acetylcholine receptors. *Sci. Rep.* **6**, 28660 (2016).
43. M. Knoll *et al*., SYK kinase mediates brown fat differentiation and activation. *Nat. Commun.* **8**, 2115 (2017).
44. M. S. Isidor *et al*., An siRNA-based method for efficient silencing of gene expression in mature brown adipocytes. *Adipocyte* **5**, 175–185 (2015).
45. G. D'Antona *et al*., Branched-chain amino acid supplementation promotes survival and supports cardiac and skeletal muscle mitochondrial biogenesis in middle-aged mice. *Cell Metab.* **12**, 362–372 (2010).
46. R Taguchi, M Ishikawa, Precise and global identification of phospholipid molecular species by an Orbitrap mass spectrometer and automated search engine Lipid Search. *J. Chromatogr. A* **1217**, 4229–4239 (2010).